This article has been accepted for publication in a future issue of this journal, but has not been fully edited. Content may change prior to final publication. Citation information: DOI 10.1109/TWC.2017.2711004, IEEE Transactions on Wireless Communications

Performance of SIM-MDPSK FSO Systems with Hardware Imperfections

Milica I. Petkovic, *Student Member, IEEE,* Goran T. Djordjevic, *Member, IEEE,* George K. Karagiannidis, *Fellow, IEEE*, and Gradimir V. Milovanovic

***Abstract*—This paper studies the error performance of free-space optical (FSO) systems, employing subcarrier intensity modulation (SIM) with M-ary differential phase-shift keying (MDPSK). Novel analytical expressions for the symbol error probability (SEP) are derived, based on the Fourier series approach. The irradiance fluctuations of the received optical signal are modeled by considering both Gamma-Gamma atmospheric turbulence and pointing errors. In addition, hardware imperfections of DPSK demodulator, as the phase noise of local oscillator at the receiver, are taken into account. It is illustrated that the phase noise significantly degrades the system performance, especially when the optical signal transmission is impaired by weak atmospheric turbulence and weak pointing errors effect. Furthermore, the phase noise results in an unrecoverable error-rate floor, which is an important limiting factor for SIM-DPSK FSO systems.**

***Index Terms*—Atmospheric turbulence, free-space optics (FSO), Gamma-Gamma distribution, differential phase-shift keying (DPSK), phase noise, subcarrier intensity modulation (SIM), symbol error probability (SEP).**

I. Introduction

BESIDES the main advantages, as high data rate, wide bandwidth and license-free transmission, free-space optical (FSO) systems are also characterized by low-power and low-cost transmission, as well as easy and simple installation. Intensity-modulation/direct detection (IM/DD) with on-off keying (OOK) is usually employed in commercial FSO systems. However, in order to improve the system performance subcarrier intensity modulation (SIM) was proposed, where the radio-frequency (RF) subcarrier signal is firstly premodulated by the data sequence bearing information, and then it is used to modulate the intensity of the laser source [1]–[4].

Several well-known modulation techniques from the field of RF communications, were used to modulate a subcarrier signal in FSO systems. The SIM based FSO system employing quadrature amplitude modulation (QAM) were analysed in [5]–[9], while SIM with M-ary phase-shift keying (MPSK) was investigated in [4], [9]–[14]. Furthermore, practical wireless communication systems also employ differential phase-shift keying (DPSK), which does not require the carrier phase estimation at the receiver. The performance of FSO systems with coherent detection and binary DPSK (BDPSK) was analyzed in [3], [15]–[19], while the case of SIM-BDPSK was investigated in [20]–[26]. Furthermore, in order to increase the capacity (or the system throughput), an FSO system based on SIM and higher-order DPSK modulation was also proposed and analyzed in [12], [13], [27]. Specifically, an expression in integral form for the bit error rate (BER) was presented in [12], [13], while [27] compares the performance of different modulation formats, including BDPSK and quaternary DPSK (QDPSK), when space diversity is used at the reception.

The FSO system performance can be notably degraded due to the hardware imperfections. For example, the effects of the imperfect reference carrier signal phase recovery on error performance of SIM-MPSK FSO systems were examined in [28], considering weak atmospheric turbulence modeled by log-normal distribution. The effect of noisy reference signal extraction on error rate degradation of coherent BPSK FSO system in strong turbulence conditions was examined in [29]. Although the DPSK receiver does not require a carrier phase estimation, the hardware imperfections of the DPSK demodulator can seriously degrade the system performance. After optical-to-electrical signal conversion in SIM-DPSK receiver, it is necessary to down-convert the received DPSK signal. In other words, a local oscillator, used in DPSK receiver for down-conversion, generates signal, which is not ideal, in the sense that phase of this signal is a random process fluctuating over time. These fluctuations, which are in the same frequency band with the useful signal, have the influence on the detection process. This undesired phase is known as a *phase noise* [30], [31].

Scanning the open literature, to the best of the authors' knowledge, the effect of hardware imperfections as the phase noise on the performance of the FSO system employing SIM-MDPSK, has not been investigated so far. In this paper, we derive novel analytical expressions for the symbol error probability (SEP) of the SIM-MDPSK based FSO system, when hardware imperfections are considered, using the Fourier series method (FSM) [32]–[35]. The impact of hardware imperfections is represented through the phase noise, which is modeled by the Tikhonov distribution [36]–[38], and is generated by the local oscillator of DPSK demodulator [30], [31], [36], [39], [40]. The intensity fluctuations of the received optical signal are assumed to originate from the combined effect of the Gamma-Gamma atmospheric turbulence and the pointing errors [16], [41]–[45]. The derived SEP expression is given in the convergent series form, whose upper bound for the truncation error is estimated. Furthermore, the derived

M. I. Petkovic and G. T. Djordjevic are with University of Nis, Faculty of Electronic Engineering, Serbia (e-mail: milica.petkovic@elfak.ni.ac.rs; goran@elfak.ni.ac.rs).

G. K. Karagiannidis is with the Aristotle University of Thessaloniki, Thessaloniki 54124, Greece (e-mail: geokarag@auth.gr).

G. V. Milovanovic is with the Mathematical Institute of Serbian Academy of Sciences and Arts (SANU), Belgrade, Serbia (e-mail: gvm@mi.sanu.ac.rs).

Manuscript received xx xx, 2016.

This article has been accepted for publication in a future issue of this journal, but has not been fully edited. Content may change prior to final publication. Citation information: DOI 10.1109/TWC.2017.2711004, IEEE Transactions on Wireless Communications

expressions are simplified, when the pointing errors effect can be neglected. Finally, numerical results are presented and validated through Monte Carlo simulations.

The rest of the paper is organized as follows. Section II describes the system and channel model, while the error analysis is provided in Section III. Numerical results with discussion are presented in Section IV and some concluding remarks are given in Section V.

II. System and channel model

The block diagram of the SIM-MDPSK FSO system is presented in Fig. 1. The information data are differently encoded and PSK is applied in an RF domain [46, p. 333]. DC bias is added to avoid clipping and distortion, and resulting signal modulates the laser output, by using SIM. The radiated optical power is given by

$$P(t) = P_t\left(1 + ms(t)\right), \tag{1}$$

where P_t represents the transmitted optical power and m denotes the modulation index ($0 < m \leq 1$). The optical transmission via free space is influenced by atmospheric turbulence and pointing errors. At the receiver, direct detection is performed, DC bias is removed and an optical-to-electrical conversion is applied via a PIN photodetector. The electrical signal at the input of DPSK demodulator is expressed as

$$r_e(t) = I\eta P_t m s(t) + n(t), \tag{2}$$

where I is a random variable (RV), which follows Gamma-Gamma distribution and represents atmospheric turbulence and pointing errors, η denotes an optical-to-electrical conversion coefficient and $n(t)$ is an additive white Gaussian noise (AWGN), with zero mean and variance, σ_n^2. Finally, the electrical signal, $r_e(t)$, is recovered by the DPSK demodulator, presented in Fig. 1, assuming that hardware imperfections exist.

A. Modeling the combined effect of atmospheric turbulence and pointing errors

The well-known Gamma-Gamma distribution is used for describing the effect of atmospheric turbulence [41], while the pointing errors effect is described by the distribution which assumes the radial displacement of laser beam at receiver experiences Rayleigh distribution, with the jitter variance σ_s^2 [42, (11)].

Based on (2), the instantaneous SNR is defined as $\gamma = I^2\eta^2 {P_t}^2 m^2/(2\sigma_n^2)$. The probability density function (PDF) of γ is [5]

$$f_\gamma(\gamma) = \frac{\xi^2}{2\Gamma(\alpha)\Gamma(\beta)\gamma} G_{1,3}^{3,0}\left(\alpha\beta\kappa\sqrt{\frac{\gamma}{\mu}}\,\middle|\, {\xi^2+1 \atop \xi^2, \alpha, \beta}\right), \tag{3}$$

where $G_{p,q}^{m,n}(\cdot)$ is the Meijer's G-function [47, (9.301)], and μ represents the average electrical SNR per symbol. The relation between μ and the average electrical SNR per bit, μ_b, is $\mu = \mu_b \log_2 M$. The average electrical SNR per bit is defined as $\mu_b = \eta^2 {P_t}^2 m^2\kappa^2 A_0^2 I_l^2/(2\sigma_n^2)$, with $\kappa = \xi^2/(\xi^2+1)$ [5]. The atmospheric turbulence parameters are denoted by α and β, while ξ and A_0 represent the pointing errors parameters.

Assuming Gaussian plane wave propagation and zero inner scale, the parameters α and β are defined as $\alpha = (\exp\left[0.49\sigma_R^2(1+1.11\sigma_R^{12/5})^{-7/6}\right] - 1)^{-1}$ and $\beta = (\exp\left[0.51\sigma_R^2(1+0.69\sigma_R^{12/5})^{-5/6}\right] - 1)^{-1}$ [1], [41], with the Rytov variance $\sigma_R^2 = 1.23C_n^2 k^{7/6}L^{11/6}$. The wave-number is $k = 2\pi/\lambda$ with the wavelength λ, L is the propagation distance, and the refractive index is denoted by C_n^2.

The pointing error represents the misalignment between the transmitter laser and the receiver photodetector. The parameter ξ is defined as the ratio between the equivalent beam radius at the receiver, $w_{L_{eq}}$, and the pointing error (jitter) standard deviation at the receiver as $\xi = w_{L_{eq}}/(2\sigma_s)$. The parameter, $w_{L_{eq}}$, depends on the beam radius at distance L, w_L, as $w_{L_{eq}}^2 = w_L^2\sqrt{\pi}\mathrm{erf}(v)/\left(2v\exp\left(-v^2\right)\right)$, $v = \sqrt{\pi}a/(\sqrt{2}w_L)$ [42], where a is the radius of a circular detector aperture, $\mathrm{erf}(\cdot)$ is the error function [47, (8.250.1)], and $A_0 = \left[\mathrm{erf}(v)\right]^2$. Next, the parameter w_L is related with the beam radius at the waist, w_0, and the radius of curvature, F_0, by $w_L = w_0((\Theta_o + \Lambda_o)(1+1.63\sigma_R^{12/5}\Lambda_1))^{1/2}$, where $\Theta_o = 1 - L/F_0$, $\Lambda_o = 2L/(kw_0^2)$, $\Lambda_1 = \Lambda_o/(\Theta_o^2 + \Lambda_o^2)$ [44].

B. Phase noise

After signal conversion from optical-to-electrical domain, classical signal detection is performed in electrical domain. During the process of down-conversion, electrical signal is multiplied by local oscillator output signal. The phase of the local oscillator signal (also known as a phase noise) is a random process fluctuating over time. Frequently local oscillator is embedded in frequency syntetyzator contained phase locked loop (PLL). The phase noise generated by PLL is well known to have a Tikhonov PDF [37, Ch. 2], [38]. Hence, the phase noise, φ, of the local oscillator is assumed to be a RV which follows Tikhonov PDF given by

$$f_\varphi(\varphi) = \frac{\exp\left(b\cos(\varphi)\right)}{2\pi I_0(b)}, \quad |\varphi| \leq \pi, \tag{4}$$

where $I_n(\cdot)$ is the nth order modified Bessel function of the first kind [47, (8.431)], $b = 1/\sigma_\varphi^2$, and σ_φ^2 is the variance of the phase noise.

Here, we use the Fourier series expansion of Tikhonov PDF, because Fourier series form is tractable for integration that will be necessary in mathematical derivations of SEP. We start with the Fourier expansion [48, (9.6.34)]

$$\mathrm{e}^{b\cos\varphi} = I_0(b) + 2\sum_{n=1}^{\infty} I_n(b)\cos(n\varphi), \quad |\varphi| \leq \pi, \tag{5}$$

for a fixed $b > 0$.

Based on the expansion in (5), it is clear that Tikhonov PDF given by (4), can be expressed in the Fourier series as

$$f_\varphi(\varphi) = \frac{1}{2\pi} + \sum_{n=1}^{\infty} c_n\cos(n\varphi), \quad |\varphi| \leq \pi, \tag{6}$$

where

$$c_n = \frac{I_n(b)}{\pi I_0(b)}. \tag{7}$$

This article has been accepted for publication in a future issue of this journal, but has not been fully edited. Content may change prior to final publication. Citation information: DOI 10.1109/TWC.2017.2711004, IEEE Transactions on Wireless Communications

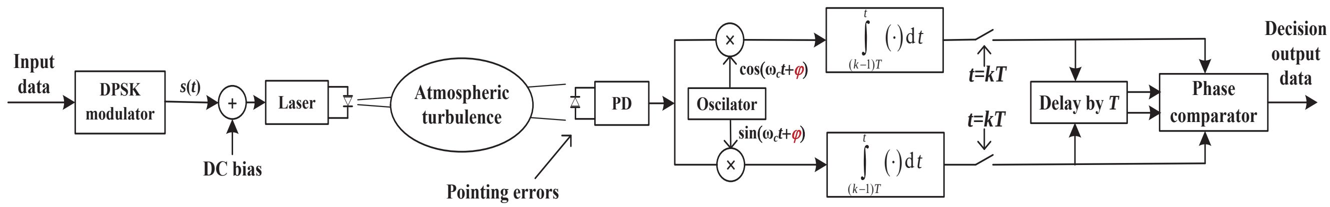

Fig. 1. Block diagram of a SIM-MDPSK FSO system

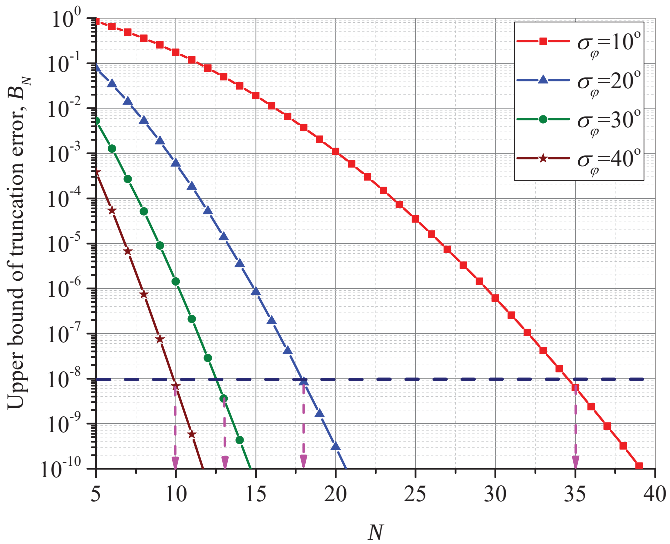

Fig. 2. Upper bound of truncation errors for $\sigma_\varphi = 10^\circ$ (*red*), $\sigma_\varphi = 20^\circ$ (*blue*), $\sigma_\varphi = 30^\circ$ (*green*), and $\sigma_\varphi = 40^\circ$ (*brown*) when $N \le 40$

Proposition 1: The series in (6) is convergent. For the truncation error

$$E_N(\varphi; b) = \sum_{n=N+1}^{\infty} c_n \cos(n\varphi), \quad |\varphi| \le \pi, \tag{8}$$

the following estimate

$$|E_N(\varphi; b)| \le E_N(0; b) \le B_N \tag{9}$$

holds, where

$$B_N \equiv B_N(b) = \frac{1}{\pi I_0(b)} \left(I_{N+1}(b) + \int_{N+1}^{\infty} I_\nu(b)\, \mathrm{d}\nu \right). \tag{10}$$

Proof: See Appendix A.

In Fig. 2, we present the bounds B_N of the truncation errors for $N \le 40$ and different values of σ_φ. If we take a threshold for the errors, e.g., $\varepsilon = 10^{-8}$ (black line in Fig. 2), so that $B_N < \varepsilon$, we see that the corresponding number of terms should be $N = 35$, 18, 13 and 10 for $\sigma_\varphi = 10^\circ, 20^\circ, 30^\circ$ and 40°, respectively.

III. Error performance

Since the decisions of the DPSK receiver are taken based on the composite phase difference between signals received during two consecutive symbol intervals, the decision variable of differential detector can be written as

$$\lambda' = [\psi_{k+1} - \psi_k] \bmod 2\pi, \tag{11}$$

where ψ_{k+1} and ψ_k are the composite phase of consecutive received signals, bearing the information at the $(k+1)$-th and the k-th interval, respectively. The local oscillator imperfections are represented through the phase noise φ_{k+1} and φ_k at the $(k+1)$-th and the k-th intervals, respectively. Then, the decision variable of the differential detector is

$$\begin{aligned} \lambda &= [(\psi_{k+1} - \varphi_{k+1}) - (\psi_k - \varphi_k)] \bmod 2\pi \\ &= [(\psi_{k+1} - \psi_k) - (\varphi_{k+1} - \varphi_k)] \bmod 2\pi. \end{aligned} \tag{12}$$

The term, $(\psi_{k+1} - \psi_k)$, represents the difference of the composite phases, while, $(\varphi_{k+1} - \varphi_k)$, denotes the impact of the phase noise.

On the contrary to the situation at the transmitter, where the phase of RF carrier is constant, the composite phase of total received signal is a RV. The PDF of the resulting phase, ψ, of received signal in a signaling interval is presented in the Fourier series form as [32]–[34]

$$f_\psi(\psi) = \frac{1}{2\pi} + \sum_{n=1}^{\infty} b_n \cos(n\psi), \tag{13}$$

where b_n represents the Fourier coefficient for the FSO channel influenced by the Gamma-Gamma atmospheric turbulence and pointing errors. In order to derive the Fourier coefficient for the considered scenario, the PDF of the received signal composite phase is written as

$$f_\psi(\psi) = \int_0^\infty f(\psi|\gamma) f_\gamma(\gamma)\, \mathrm{d}\gamma \tag{14}$$

where $f_\gamma(\gamma)$ is the PDF of the instantaneous SNR given in (3). The conditional PDF is defined through a Fourier series form of the received signal composite phase due to additive noise as [32]–[34]

$$f(\psi|\gamma) = \frac{1}{2\pi} + \sum_{n=1}^{\infty} a_n(\gamma) \cos(n\psi), \tag{15}$$

where $a_n(\gamma)$ denotes the Fourier coefficient for AWGN channel defined as [34]

$$a_n(\gamma) = \frac{\Gamma\left(\frac{n}{2}+1\right)}{n!\pi} \gamma^{\frac{n}{2}} \exp(-\gamma)\, {}_1F_1\left(\frac{n}{2}+1; n+1; \gamma\right), \tag{16}$$

where ${}_1F_1(\cdot;\cdot;\cdot)$ is the confluent hypergeometric function [47, (9.21)].

This article has been accepted for publication in a future issue of this journal, but has not been fully edited. Content may change prior to final publication. Citation information: DOI 10.1109/TWC.2017.2711004, IEEE Transactions on Wireless Communications

Proposition 2: After substituting (3), (15) and (16) into (14), the PDF of the phase ψ is given as

$$\begin{aligned} f_\psi(\psi) = {} & \frac{1}{2\pi} + \sum_{n=1}^{\infty} \frac{n 2^{\alpha+\beta-4} \xi^2}{\pi^2 \Gamma(\alpha)\Gamma(\beta)} \cos(n\psi) \\ & \times G_{3,6}^{6,1}\left(\frac{\alpha^2\beta^2\kappa^2}{16\mu} \middle| \begin{smallmatrix} 1-\frac{n}{2}, 1+\frac{n}{2}, \frac{\xi^2+2}{2} \\ \frac{\xi^2}{2}, \frac{\alpha}{2}, \frac{\alpha+1}{2}, \frac{\beta}{2}, \frac{\beta+1}{2}, 0 \end{smallmatrix} \right). \end{aligned} \tag{17}$$

Proof: See Appendix B.

Based on (13) and (17), the Fourier coefficient for FSO channel influenced by Gamma-Gamma atmospheric turbulence and pointing errors is determined as

$$\begin{aligned} b_n = {} & \frac{n 2^{\alpha+\beta-4} \xi^2}{\pi^2 \Gamma(\alpha)\Gamma(\beta)} \\ & \times G_{3,6}^{6,1}\left(\frac{\alpha^2\beta^2\kappa^2}{16\mu} \middle| \begin{smallmatrix} 1-\frac{n}{2}, 1+\frac{n}{2}, \frac{\xi^2+2}{2} \\ \frac{\xi^2}{2}, \frac{\alpha}{2}, \frac{\alpha+1}{2}, \frac{\beta}{2}, \frac{\beta+1}{2}, 0 \end{smallmatrix} \right). \end{aligned} \tag{18}$$

When the considered scenario assumes the pointing errors to be very small, it can be neglected ($\xi \to \infty$). In this case, the optical link suffers only from atmospheric turbulence, and the Fourier coefficient can be found by taking the limit of (18) for $\xi \to \infty$. After applying [49, (07.34.25.0007.01), (07.34.25.0006.01) and (06.05.16.0002.01)], the Fourier coefficient can be derived as

$$\begin{aligned} b_n^{GG} = \lim_{\xi\to\infty} b_n = {} & \frac{n 2^{\alpha+\beta-3}}{\pi^2 \Gamma(\alpha)\Gamma(\beta)} \\ & \times G_{2,5}^{5,1}\left(\frac{\alpha^2\beta^2}{16\mu} \middle| \begin{smallmatrix} 1-\frac{n}{2}, 1+\frac{n}{2} \\ \frac{\alpha}{2}, \frac{\alpha+1}{2}, \frac{\beta}{2}, \frac{\beta+1}{2}, 0 \end{smallmatrix} \right). \end{aligned} \tag{19}$$

For further analysis, it is required to find the PDF of the decision variable λ, defined in (12). Firstly, we will introduce the following rule related to the PDFs presented in the Fourier series form.

Proposition 3: If the variables x_1 and x_2 are RVs with the PDFs given in the Fourier series form, with coefficients z_{1n} and z_{2n}, respectively, as

$$\begin{aligned} f_{x_1}(x) &= \frac{1}{2\pi} + \sum_{n=1}^{\infty} z_{1n} \cos(nx), \quad |x| \le \pi, \\ f_{x_2}(x) &= \frac{1}{2\pi} + \sum_{n=1}^{\infty} z_{2n} \cos(nx), \quad |x| \le \pi, \end{aligned} \tag{20}$$

then, the PDF of $y = [x_1 - x_2] \bmod 2\pi$, is

$$f_y(y) = \frac{1}{2\pi} + \sum_{n=1}^{\infty} \pi z_{1n} z_{2n} \cos(ny), \quad |y| \le \pi. \tag{21}$$

Proof: The proof can be found in [36], [50], [51].

A. Error analysis without considering hardware imperfections

If no hardware imperfections are assumed, the decision variable λ' is defined in (11). Based on Proposition 3, after replacing x_1 and x_2 with ψ_{k+1} and ψ_k, respectively, and both z_{1n} and z_{2n} with b_n, the PDF of λ' can be easily obtained as

$$f_{\lambda'}(\lambda') = \frac{1}{2\pi} + \sum_{n=1}^{\infty} \pi b_n^2 \cos(n\lambda'), \quad |\lambda'| \le \pi. \tag{22}$$

The detection is performed in the manner to find the closest possible transmitted phase compared with received composite phase λ' . The probability of wrong symbol detection is given by

$$P_s = 1 - \int_{-\pi/M}^{\pi/M} f_{\lambda'}(\lambda')\, \mathrm{d}\lambda'. \tag{23}$$

By substituting (22) into (23), the average SEP can be found as

$$P_s = 1 - \frac{1}{M} - \sum_{n=1}^{\infty} \frac{2\pi b_n^2}{n} \sin\left(\frac{n\pi}{M}\right). \tag{24}$$

In [13], an expression for the average BER was derived in integral form, assuming that the intensity fluctuations of the optical signal are modeled by the log-normal and Gamma-Gamma distributions. In the region of high average electrical SNR values, the bit error probability could be approximated by $BER \approx P_s/\log_2 M$ [40, p. 271]. By using this approximation and SEP in (24) with the Fourier coefficient of (19), the numerical results from [13, Fig. 2] can be obtained.

B. Error analysis in the presence of phase noise

In the presence of the phase noise, the decision variable λ is defined as in (12). The PDF of the variable, $\delta = \varphi_{k+1} - \varphi_k$, can be found by utilization of Proposition 3. Since the Tikhonov PDF of the phase noise is given in the Fourier series form by (6), the PDF of the variable δ is found as

$$f_\delta(\delta) = \frac{1}{2\pi} + \sum_{n=1}^{\infty} \pi c_n^2 \cos(n\delta), \quad |\delta| \le \pi, \tag{25}$$

with the Fourier coefficient c_n previously defined by (7).

Taking into consideration that the variables ψ and φ are statistically independent, based on (22) and (25), and Proposition 3, the PDF of λ is

$$f_\lambda(\lambda) = \frac{1}{2\pi} + \sum_{n=1}^{\infty} \pi^3 b_n^2 c_n^2 \cos(n\lambda), \quad |\lambda| \le \pi. \tag{26}$$

When the Gamma-Gamma atmospheric turbulence, pointing errors and phase noise are assumed, the average SEP of the SIM-MDPSK FSO system can be written as

$$\begin{aligned} P_s &= 1 - \int_{-\pi/M}^{\pi/M} f_\lambda(\lambda)\, \mathrm{d}\lambda \\ &= 1 - \frac{1}{M} - \sum_{n=1}^{\infty} \frac{2\pi^3 b_n^2 c_n^2}{n} \sin\left(\frac{n\pi}{M}\right), \end{aligned} \tag{27}$$

where the Fourier coefficients b_n and c_n are previously defined in (18) and (7), respectively.

Proposition 4: The series in (27) is convergent and the following estimate

$$\left| P_s - 1 + \frac{1}{M} + \sum_{n=1}^{N} \frac{2\pi^3 b_n^2 c_n^2}{n} \sin\left(\frac{n\pi}{M}\right) \right| \le E_N^{\mathrm{SEP}} \tag{28}$$

This article has been accepted for publication in a future issue of this journal, but has not been fully edited. Content may change prior to final publication. Citation information: DOI 10.1109/TWC.2017.2711004, IEEE Transactions on Wireless Communications

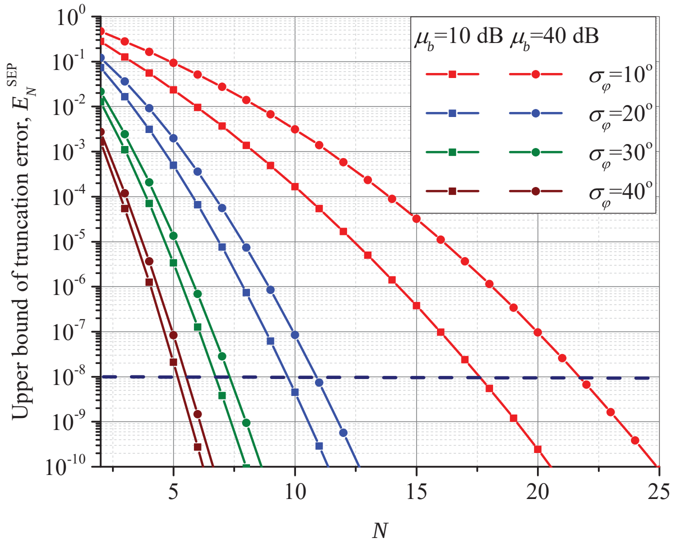

Fig. 3. Upper bound of truncation errors for $\sigma_\varphi = 10°$ (*red*), $\sigma_\varphi = 20°$ (*blue*), $\sigma_\varphi = 30°$ (*green*), and $\sigma_\varphi = 40°$ (*brown*) when $N \leq 25$

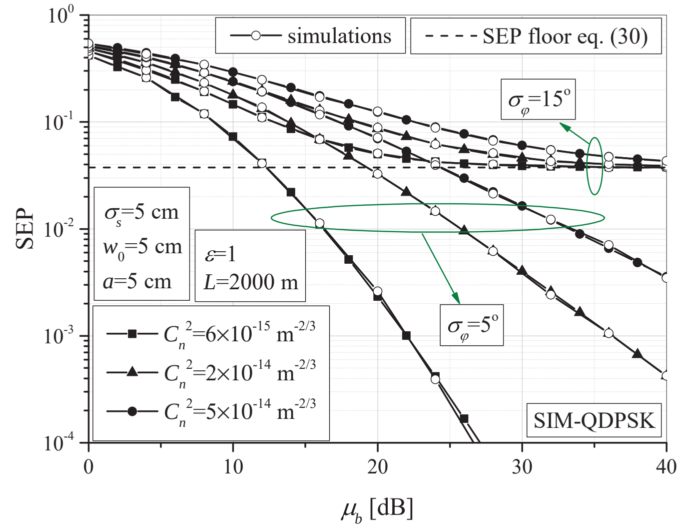

Fig. 4. SIM-QDPSK SEP versus average electrical SNR for different values of the phase noise standard deviation in various atmospheric turbulence conditions

holds, with the bound of truncation error

$$E_N^{\mathrm{SEP}} = \frac{2\pi b_{N+1}^2}{I_0(b)^2}\left(\frac{I_{N+1}(b)^2}{N+1} + \int_{N+1}^{\infty}\frac{I_\nu(b)^2}{\nu}\,\mathrm{d}\nu\right). \quad (29)$$

Proof: See Appendix C.

This truncation error is illustrated in Fig. 3. To achieve the given truncation error, the higher number of terms in summation is required if the standard deviation is lower. In order to achieve truncation error less than 10^{-8}, for $\mu = 10$ dB the required number of terms in summation is $N = 18, 10, 7$ and 6, when $\sigma_\varphi = 10^o, 20^o, 30^o$ and 40^o, respectively. In addition, the convergence rate decreases with increasing the electrical SNR. In other words, the proposed series expression converges better in low electrical SNR regime compared to high electrical SNR regime.

As it will be shown in the next Section, the existence of the phase noise results in the unrecoverable error-rate floor, which is a meaningful limiting factor in SIM-DPSK based FSO systems. This error-rate floor represents the constant value of the average SEP, which occurs at the high average electrical SNR. With a further increase in the transmitted optical power, the improvement of the SEP performance will not be achieved.

Proposition 5: The unrecoverable error-rate floor can be expressed as

$$P_s^{floor} = 1 - \frac{1}{M} - \sum_{n=1}^{\infty}\frac{2\pi c_n^2}{n}\sin\left(\frac{n\pi}{M}\right). \quad (30)$$

Proof: See Appendix D.

It can be noticed that the SEP floor is independent on the FSO channel state (atmospheric turbulence and pointing errors). On the other hand, the value of the SEP floor depends on the phase noise standard deviation and order of DPSK modulation, as it will be presented in the next Section.

IV. Numerical results and discussion

Based on derived expressions for the average SEP, numerical results are obtained and validated by Monte Carlo simulations. Monte Carlo simulations have been performed using MATLAB® software package. Since intensity fluctuations originate from both atmospheric turbulence and pointing errors, the resulting optical signal intensity, I, is obtained as a product of two different RVs, i.e., $I = I_a \times I_p$. The intensity fluctuations, I_a, due to atmospheric turbulence are modeled by Gamma-Gamma distribution. The corresponding RV, I_a, is generated as a product of two independent Gamma-distributed RVs with shaping parameters α and β. Command for generating Gamma-distributed RV is built-in into MATLAB®. The RVs relating to the pointing errors, I_p, are generated based on [42, (9)], employing built-in command for generating Rayleigh RV. The Tikhonov-distributed samples of phase noise are generated using the modified acceptance/rejection method, explained in [52, p. 382]. Modulation and demodulation is simulated based on [46, p. 333-335]. The average SEP values are estimated using 10^7 transmitted symbols.

In order to obtain the numerical results, the atmospheric turbulence strength is determined by the refractive index structure parameter as: $C_n^2 = 6 \times 10^{-15}$ m$^{-2/3}$ for weak, $C_n^2 = 2 \times 10^{-14}$ m$^{-2/3}$ for moderate and $C_n^2 = 5 \times 10^{-14}$ m$^{-2/3}$ for strong turbulence conditions. The impact of the phase noise is specified by the phase noise standard deviation.

The average SEP dependence on the average electrical SNR of the FSO system employing SIM-QDPSK is presented in Fig. 4, assuming different atmospheric turbulence conditions and phase noise standard deviation $\sigma_\varphi = 5^o$ or $\sigma_\varphi = 15^o$. Lower values of the phase noise standard deviation correspond to the weaker phase noise and better system performance. Furthermore, the impact of the atmospheric turbulence conditions is stronger when the value of σ_φ is lower. On the other hand, when the effect of phase noise is very strong, the atmospheric turbulence conditions has minor influence on the SEP performance. In addition, the existence of the unrecoverable error-rate floor is noticed in Fig. 4, meaning that the DPSK hardware imperfections presented through phase

This article has been accepted for publication in a future issue of this journal, but has not been fully edited. Content may change prior to final publication. Citation information: DOI 10.1109/TWC.2017.2711004, IEEE Transactions on Wireless Communications

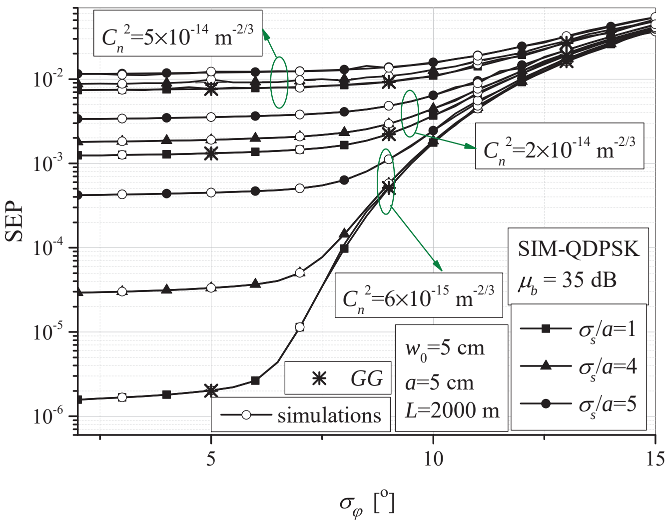

Fig. 5. SIM-QDPSK SEP versus the phase noise standard deviation for different values of the normalized jitter standard deviation, in various atmospheric turbulence conditions

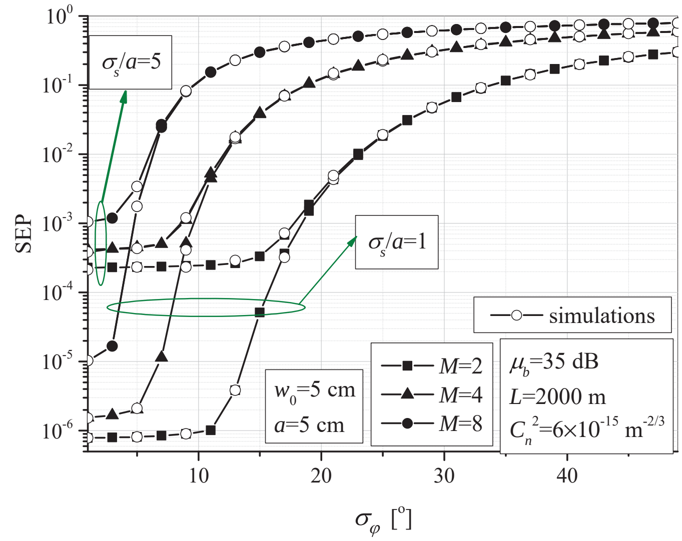

Fig. 6. SIM-MDPSK SEP versus the phase noise standard deviation for different values of the normalized jitter standard deviations

noise are an important limiting factor for SIM-DPSK systems.

This SEP floor appears at lower values of average electrical SNR in weak atmospheric turbulence, as well as when the value of σ_φ is greater (stronger impact of the phase noise). The SEP floor results based on (30) for $\sigma_\varphi = 5^o$ are not visible in Fig. 4 due to very low value. It can be concluded that the SEP floor is not dependent on atmospheric turbulence conditions, which is in agreement with mathematical derivation (see (41) and (30)).

Fig. 5 presents the SIM-QDPSK SEP dependence on the phase noise standard deviation for different values of the normalized jitter standard deviation, in various atmospheric turbulence conditions. It can be observed that lower values of the normalized jitter standard deviation reflects in better system performance. It means that the positioning of the FSO apertures is better and the pointing errors effect is weaker. Also, the pointing error effect is stronger in weak compared to moderate and strong atmospheric turbulence. When the optical signal transmission suffers from very strong atmospheric turbulence, the pointing errors effect has less impact on the SEP performance.

In addition, the results for the FSO system when the pointing errors effect is neglected, obtained by using (27) and (19), are also presented. These results are in agreement with those when $\sigma_s/a = 1$. Hence, very low values of the normalized jitter standard deviation means that the pointing errors effect is very weak and can be neglected.

When the DPSK demodulator hardware imperfections are dominant, and the phase noise is quite strong, the value of σ_φ is large. In that case, the FSO channel state (atmospheric turbulence and pointing errors) does not play a major role in the SEP performance. When $\sigma_\varphi \to 0$, the impact of the phase noise is very weak and can be neglected. For these phase noise standard deviation values, the SEP takes constant values, which are approximately the same as the SEP values for the FSO system without phase noise. Also, atmospheric turbulence and pointing errors have very strong impact on the

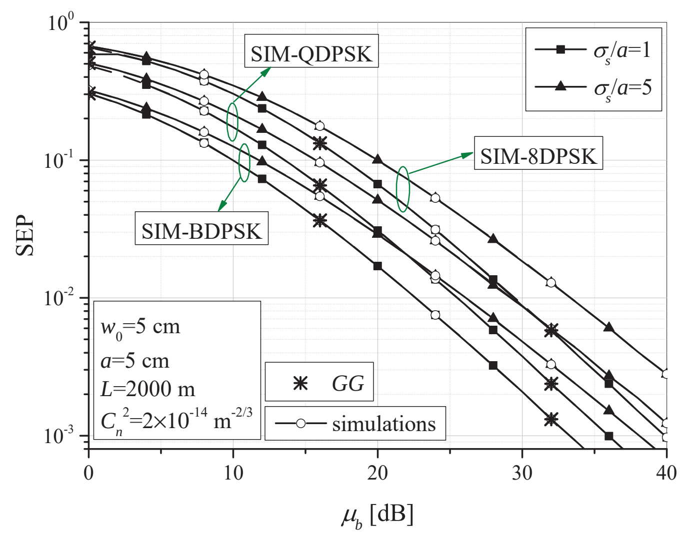

Fig. 7. SIM-MDPSK SEP versus average electrical SNR of the FSO system without hardware imperfections

SEP performance, when σ_φ is low.

Fig. 6 represents the SIM-MDPSK SEP dependence on the phase noise standard deviation. The impact of the phase noise on SEP is stronger when higher order SIM-MDPSK is employed. For example, for $\sigma_s/a = 1$, in the case of $M = 2$, the SEP is independent on phase noise up to $\sigma_\varphi = 10^o$, while for $M = 8$, SEP drastically increases even starting from $\sigma_\varphi = 2^o$. In addition, the weaker the pointing errors, the stronger is the effect of phase noise on SEP. It can be observed that the efect of DPSK order has minor influence on the SEP performance when the impact of the phase noise is very strong.

The SEP dependence on the average electrical SNR of the FSO system without hardware imperfections is presented in Fig. 7. The results are obtained based on (24) with the Fourier coefficient in (18), or in (19) when the pointing errors are neglected. Different DPSK formats are observed: SIM employing BDPSK, QDPSK and 8DPSK. As it is expected, FSO system based on SIM-DPSK with higher modulation format has worse SEP performance, but the larger amount of information can be transmitted. Also, consistent with previous conclusions, greater value of the normalized jitter standard deviations means worse system performance due to stronger pointing errors. Agreement of the results based on (18) for $\sigma_s/a = 1$ and (19) is noticed, meaning that very low jitter standard deviation leads to weak pointing errors.

V. Conclusion

We have derived novel analytical expressions for the average SEP of FSO system employing SIM-MDPSK. The irradiance fluctuations at the received signal originate from the Gamma-Gamma atmospheric turbulence and pointing errors. Based on derived SEP expressions, numerical results have been presented and confirmed by Monte Carlo simulations.

From the illustrated results, we have found that the hardware imperfections result in the significant deterioration of the FSO system performance. The phase noise is dominant system factor, which causes the SEP performance damaging, especially when optical signal transmission is influenced by favorable conditions (weak atmospheric turbulence and weak pointing errors effect). Similarly, when the impact of the phase noise is very strong, atmospheric turbulence and pointing errors effect has minor effect on the system performance. Furthermore, the SIM based FSO system with higher DPSK format is more sensitive to the existence of the phase noise. Further, the existence of the phase noise leads to the unrecoverable SEP floor, being meaningful limiting factor for SIM-DPSK systems. It is observed that the SEP floor is not dependent on the FSO channel state, but it is highly dependent on the phase noise standard deviation and the DPSK modulation order.

Appendix A
Proof of Proposition 1

The series in (6) is a uniformly convergent series, because the numerical series with positive terms,

$$\sum_{n=1}^{\infty} I_n(b), \tag{31}$$

is convergent, which can be proved using the inequality [53]

$$\left(1+\frac{\nu}{b}\right) I_{\nu+1}(b) < I_\nu(b) \quad (\nu \geq -1,\ b>0). \tag{32}$$

Namely, the series (31) is convergent if for a fixed $m = \lceil b \rceil$ ($\lceil x \rceil$ denotes the smallest integer greater than or equal to x) the series $\sum\limits_{n=m}^{\infty} I_n(b)$ converges. According to (32), for $n > m$ we have

$$I_n(b) < \frac{I_{n-1}(b)}{1+(n-1)/b} < \frac{I_{n-1}(b)}{2} < \cdots < \frac{I_m(b)}{2^{n-m}}, \tag{33}$$

so that

$$\sum_{n=m}^{\infty} I_n(b) < I_m(b) \sum_{n=m}^{\infty} \frac{1}{2^{n-m}} = 2I_m(b),$$

wherefrom we conclude that the series $\sum\limits_{n=m}^{\infty} I_n(b)$ and (31) are convergent. The sum of (31) is $S = \frac{1}{2}(\mathrm{e}^b - I_0(b))$ [54, p. 254].

According to Cauchy's integral test (cf. [55, p. 120] or [56, p. 159]), for the numerical series (31) we can give the following estimates for the remainder term

$$\sum_{n=N+1}^{\infty} I_n(b) \leq I_{N+1}(b) + \int_{N+1}^{\infty} I_\nu(b)\,\mathrm{d}\nu, \tag{34}$$

where $\nu \mapsto I_\nu(a)$ is a decreasing positive continuous function on $(0,\infty)$ [53].

Thus, for the truncation error $E_N(\varphi;b)$ given by (8) we obtain $|E_N(\varphi;b)| \leq E_N(0;b) = (\pi I_0(b))^{-1}\sum_{n=N+1}^{\infty} I_n(b)$, i.e., (9), where B_N is given by (10), because of (34).

Appendix B
Proof of Proposition 2

After substituting (3), (15) and (16) into (14), the PDF of the phase ψ is re-written as

$$\begin{aligned} f_\psi(\psi) &= \frac{1}{2\pi} + \sum_{n=1}^{\infty} \frac{\Gamma\left(\frac{n}{2}+1\right)}{n!\pi} \frac{\xi^2}{2\Gamma(\alpha)\Gamma(\beta)} \cos(n\psi) \\ &\times \int_0^{\infty} \gamma^{\frac{n}{2}-1} \exp(-\gamma)\, {}_1F_1\left(\frac{n}{2}+1; n+1; \gamma\right) \\ &\times G_{1,3}^{3,0}\left(\alpha\beta\kappa\sqrt{\frac{\gamma}{\mu}} \,\middle|\, \begin{matrix} \xi^2+1 \\ \xi^2, \alpha, \beta \end{matrix}\right) \mathrm{d}\gamma. \end{aligned} \tag{35}$$

Based on [49, (07.20.26.0015.01)], the product of exponential and confluent hypergeometric function is presented in terms of the Meijer's G-function as

$$\exp(-\gamma)\,{}_1F_1\left(\frac{n}{2}+1; n+1; \gamma\right) = \frac{\Gamma(n+1)}{\Gamma\left(\frac{n}{2}\right)} G_{1,2}^{1,1}\left(\gamma \,\middle|\, \begin{matrix} 1-\frac{n}{2} \\ 0, -n \end{matrix}\right). \tag{36}$$

After substituting (36) into (35) and applying [49, (06.05.16.0002.01) and (06.05.03.0001.01)], the PDF of the phase ψ is

$$\begin{aligned} f_\psi(\psi) &= \frac{1}{2\pi} + \sum_{n=1}^{\infty} \frac{n\xi^2}{4\pi\Gamma(\alpha)\Gamma(\beta)} \cos(n\psi) \\ &\times \int_0^{\infty} \gamma^{\frac{n}{2}-1} G_{1,2}^{1,1}\left(\gamma \,\middle|\, \begin{matrix} 1-\frac{n}{2} \\ 0, -n \end{matrix}\right) G_{1,3}^{3,0}\left(\alpha\beta\kappa\sqrt{\frac{\gamma}{\mu}} \,\middle|\, \begin{matrix} \xi^2+1 \\ \xi^2, \alpha, \beta \end{matrix}\right) \mathrm{d}\gamma. \end{aligned} \tag{37}$$

The integral in (37) can be evaluated in closed-form by using [49, (07.34.21.0013.01)], so the PDF of the phase ψ is derived as

$$\begin{aligned} f_\psi(\psi) &= \frac{1}{2\pi} + \sum_{n=1}^{\infty} \frac{n2^{\alpha+\beta-4}\xi^2}{\pi^2\Gamma(\alpha)\Gamma(\beta)} \cos(n\psi) \\ &\times G_{4,7}^{7,1}\left(\frac{\alpha^2\beta^2\kappa^2}{16\mu} \,\middle|\, \begin{matrix} 1-\frac{n}{2}, 1+\frac{n}{2}, \frac{\xi^2+2}{2}, \frac{\xi^2+2}{2} \\ \frac{\xi^2}{2}, \frac{\xi^2+1}{2}, \frac{\alpha}{2}, \frac{\alpha+1}{2}, \frac{\beta}{2}, \frac{\beta+1}{2}, 0 \end{matrix}\right). \end{aligned} \tag{38}$$

After the permutation of the parameters via [49, (07.34.04.0003.01) and (07.34.04.0004.01)], and the transformation of the Meijer's G-function by [49, (07.34.03.0002.01)], the final form of the PDF of the phase ψ is presented in (17).

APPENDIX C
PROOF OF PROPOSITION 4

We observe the series in (27) given by

$$S = \sum_{n=1}^{\infty} \frac{2\pi^3 b_n^2 c_n^2}{n} \sin\left(\frac{n\pi}{M}\right), \tag{39}$$

for which we can prove its absolute convergence. As in APPENDIX A we use the inequalities (32) and (33) and consider the series $\sum\limits_{n=m}^{\infty} 2\pi^3 b_n^2 c_n^2/n$, where $m = \lceil b \rceil$. Since b_n is a decreasing sequence, we can write

$$\sum_{n=m}^{\infty} \frac{2\pi^3 b_n^2 c_n^2}{n} < 2\pi^3 b_m^2 \sum_{n=m}^{\infty} \frac{c_n^2}{n} = \frac{2\pi b_m^2}{I_0(b)^2} \sum_{n=m}^{\infty} \frac{I_n(b)^2}{n}.$$

Now, using (33) we conclude that

$$\sum_{n=m}^{\infty} \frac{I_n(b)^2}{n} < I_m(b)^2 \sum_{n=m}^{\infty} \frac{1}{n 4^{n-m}} < \frac{4 I_m(b)^2}{3m},$$

i.e.,

$$\sum_{n=m}^{\infty} \frac{2\pi^3 b_n^2 c_n^2}{n} < \frac{8\pi b_m^2}{3m} \left(\frac{I_m(b)}{I_0(b)}\right)^2 < +\infty.$$

Thus, the series (39) is absolutely convergent, and also convergent. For its truncation error we obtain the following estimate

$$\begin{aligned} \left| \sum_{n=N+1}^{\infty} \frac{2\pi^3 b_n^2 c_n^2}{n} \sin\left(\frac{n\pi}{M}\right) \right| &\le \sum_{n=N+1}^{\infty} \frac{2\pi^3 b_n^2 c_n^2}{n} \\ &\le \frac{2\pi b_{N+1}^2}{I_0(b)^2} \sum_{n=N+1}^{\infty} \frac{I_n(b)^2}{n}. \end{aligned}$$

Based on Cauchy's criteria, as in APPENDIX A, it follows

$$\sum_{n=N+1}^{\infty} \frac{I_n(b)^2}{n} \le \frac{I_{N+1}(b)^2}{N+1} + \int_{N+1}^{\infty} \frac{I_\nu(b)^2}{\nu}\, \mathrm{d}\nu$$

so that we get (28), with (29).

APPENDIX D
PROOF OF PROPOSITION 5

In order to determine the value of the SEP floor, it is necessary to take the limit of (27) for $\mu \to \infty$, i.e.,

$$P_s^{floor} = \lim_{\mu\to\infty} P_s = \lim_{\mu\to\infty} \left\{ 1 - \frac{1}{M} - \sum_{n=1}^{\infty} \frac{2\pi^3 b_n^2 c_n^2}{n} \sin\left(\frac{n\pi}{M}\right) \right\}. \tag{40}$$

Since the Fourier coefficient b_n is the only term in (27), which depends on the average electrical SNR, after following derivation in this Appendix, the limit of b_n for $\mu \to \infty$ is derived as

$$b_n^{\mu\to\infty} = \lim_{\mu\to\infty} b_n = \frac{1}{\pi}. \tag{41}$$

The term $b_n^{\mu\to\infty}$ is derived by following

$$\begin{aligned} \lim_{\mu\to\infty} b_n &= \lim_{\mu\to\infty} \frac{n 2^{\alpha+\beta-4} \xi^2}{\pi^2 \Gamma(\alpha) \Gamma(\beta)} \\ &\times G_{3,6}^{6,1}\left(\frac{\alpha^2\beta^2\kappa^2}{16\mu} \middle| \begin{smallmatrix} 1-\frac{n}{2}, 1+\frac{n}{2}, \frac{\xi^2+2}{2} \\ \frac{\xi^2}{2}, \frac{\alpha}{2}, \frac{\alpha+1}{2}, \frac{\beta}{2}, \frac{\beta+1}{2}, 0 \end{smallmatrix} \right) \\ &= \lim_{z\to 0} \frac{n 2^{\alpha+\beta-4} \xi^2}{\pi^2 \Gamma(\alpha) \Gamma(\beta)} \\ &\times G_{3,6}^{6,1}\left(z \middle| \begin{smallmatrix} 1-\frac{n}{2}, 1+\frac{n}{2}, \frac{\xi^2+2}{2} \\ \frac{\xi^2}{2}, \frac{\alpha}{2}, \frac{\alpha+1}{2}, \frac{\beta}{2}, \frac{\beta+1}{2}, 0 \end{smallmatrix} \right). \end{aligned} \tag{42}$$

The first step in finding $\lim\limits_{\mu\to\infty} b_n$ is applying [49, (07.34.06.0001.01)] to represent the Meijer's *G*-function in (42) in series form. Since $z \to 0$, higher order terms in the series representation of Meijer's *G*-function can be neglected, and $b_n^{\mu\to\infty}$ is determined as

$$\begin{aligned} b_n^{\mu\to\infty} &= \lim_{\mu\to\infty} b_n \approx \frac{1}{2^2\pi^2} \\ &\times \frac{2^\alpha \Gamma\left(\frac{\alpha}{2}\right) \Gamma\left(\frac{\alpha+1}{2}\right)}{\Gamma(\alpha)} \frac{2^\beta \Gamma\left(\frac{\beta}{2}\right) \Gamma\left(\frac{\beta+1}{2}\right)}{\Gamma(\beta)}. \end{aligned} \tag{43}$$

After utilizing [49, (06.05.03.0002.01) and (06.01.16.0006.01)], it is proved that holds

$$\frac{2^x \Gamma\left(\frac{x}{2}\right) \Gamma\left(\frac{x+1}{2}\right)}{\Gamma(x)} = 2\sqrt{\pi}, \tag{44}$$

so the final form of $b_n^{\mu\to\infty}$ is derived as

$$b_n^{\mu\to\infty} = \frac{1}{\pi}. \tag{45}$$

ACKNOWLEDGMENT

This paper was supported by Ministry of Foreign Affairs of Norway within the NORBAS project, the Ministry of Education, Science and Technology Development of Republic of Serbia under grants TR-32028 and IO-174015 and the Serbian Academy of Sciences and Arts (No. Φ-96).

REFERENCES

[1] Z. Ghassemlooy, W. Popoola, and S. Rajbhandari, *Optical Wireless Communications: System and Channel Modelling With MATLAB®*. Boca Raton, FL, USA: CRC Press, 2013.

[2] S. Arnon, J. Barry, G. Karagiannidis, R. Schober, and M. Uysal, Eds., *Advanced Optical Wireless Communication Systems*. New York, USA: Cambridge University Press, 2012.

[3] M. Niu, J. Cheng, and J. F. Holzman, "Error rate performance comparison of coherent and subcarrier intensity modulated optical wireless communications," *IEEE/OSA J. Opt. Commun. Netw.*, vol. 5, no. 6, pp. 554–564, Jun. 2013.

[4] J. Li, J. Q. Liu, and D. P. Taylor, "Optical communication using subcarrier PSK intensity modulation through atmospheric turbulence channels," *IEEE Trans. Commun.*, vol. 55, no. 8, pp. 1598–1606, Aug. 2007.

[5] G. T. Djordjevic and M. I. Petkovic, "Average BER performance of FSO SIM-QAM systems in the presence of atmospheric turbulence and pointing errors", *J. Mod. Opt.,* vol. 63, no. 8, pp. 715-723, Oct. 2015.

[6] M. Z. Hassan, X. Song, and J. Cheng, "Subcarrier intensity modulated wireless optical communications with rectangular QAM," *IEEE/OSA J. Opt. Commun. Netw.*, vol. 4, no. 6, pp. 522-532, Jun. 2012.

[7] K. P. Peppas and C. K. Datsikas, "Average symbol error probability of general-order rectangular quadrature amplitude modulation of optical wireless communication systems over atmospheric turbulence channels," *IEEE/OSA J. Opt. Commun. Netw.*, vol. 2, no. 2, pp. 102-110, Feb. 2010.

This article has been accepted for publication in a future issue of this journal, but has not been fully edited. Content may change prior to final publication. Citation information: DOI 10.1109/TWC.2017.2711004, IEEE Transactions on Wireless Communications

[8] H. D. Trung, D. T. Tuan, and A. T. Pham, ”Pointing error effects on performance of free-space optical communication systems using SC–QAM signals over atmospheric turbulence channels,” *International Journal of Electronics and Communications (AEÜ)*, vol. 68, no. 9, pp. 869-876, Sep. 2014.

[9] P. K. Sharma, A. Bansal, and P. Garg, ”Relay assisted bi-directional communication in generalized turbulence fading,” *J. Lightw. Technol.*, vol. 33, no. 1, pp. 133-139, Jan. 2015.

[10] P. K. Sharma, and P. Garg, ”Bi-directional decode-XOR-forward relaying over M-distributed free space optical links,” *IEEE Photon. Technol. Lett.*, vol. 26, no. 19, pp. 1916-1919, Oct. 2014.

[11] X. Song, M. Niu, and J. Cheng, ”Error rate of subcarrier intensity modulations for wireless optical communications,” *IEEE Commun. Lett.*, vol. 16, no. 4, pp. 540-543, Apr. 2012.

[12] X. Song, F. Yang, J. Cheng, and M.−S. Alouni, ”Subcarrier MPSK/MDPSK modulated optical wireless communications in lognormal turbulence,” in *Proc. WCNC 2015*, New Orleans, LA, pp. 41-45, March 912, 2015.

[13] X. Song, F. Yang, J. Cheng, and M.−S. Alouini, ”BER of subcarrier MPSK and MDPSK systems in atmospheric turbulence,” *J. Lightw. Technol.*, vol. 33, no. 1, pp. 161–170, Jan. 2015.

[14] N. D. Chatzidiamantis, A. S. Lioumpas, G. K. Karagiannidis, and S. Arnon, ”Adaptive subcarrier PSK intensity modulation in free space optical systems,” *IEEE Trans. Commun.*, vol. 59, no. 5, pp. 1368-1377, May 2011.

[15] K. Kiasaleh, ”Performance of coherent DPSK free-space optical communication systems in K-distributed turbulence,” *IEEE Trans. Commun.*, vol. 54, no. 4, pp. 604–607, Apr. 2006.

[16] H. G. Sandalidis, T. A. Tsiftsis, and G. K. Karagiannidis, ”Optical wireless communications with heterodyne detection over turbulence channels with pointing errors,” *J. Lightw. Technol.*, vol. 27, no. 20, pp. 4440–4445, Oct. 2009.

[17] M. Niu, J. Cheng, J. F. Holzman, and L. McPhail, ”Performance analysis of coherent free space optical communication systems with K-distributed turbulence,” in *Proc. ICC 2009*, Dresden, pp. 1–5, Jun. 2009.

[18] M. Niu, X. Song, J. Cheng, and J. F. Holzman, ”Performance analysis of coherent wireless optical communications with atmospheric turbulence,” *Opt. express*, vol. 20, no. 6, pp. 6515–6520, Mar. 2012.

[19] H. Samimi and M. Uysal, ”Performance of coherent differential phase-shift keying free-space optical communication systems in M-distributed turbulence,” *IEEE/OSA J. Opt. Commun. Netw.*, vol. 5, no. 7, pp. 704–710, Jul. 2013.

[20] K. Prabu, P. P. Bharati, and D. S. Kumar, ”Performance analysis of DPSK-SIM based FSO system over strong atmospheric turbulence channel,” in *Proc. 2013 INDICON*, Mumbai, pp. 1-4, Dec. 2013.

[21] K. Prabu and S. Kumar, ”BER analysis of DPSK-SIM over MIMO free space optical links with misalignment,” *Optik*, vol. 125, no. 18, pp. 5176-5180, Sep. 2014.

[22] Z. Gao, H. Liu, R. Liao, and X. Ma, ”Performance of free-space optical communication system using differential phase-shift keying subcarrier-intensity modulated over the exponentiated Weibull channel,” *Opt. Eng.*, vol. 54, no. 10, pp. 106109-1–106109-8, Oct. 2015.

[23] W. O. Popoola, Z. Ghassemlooy, and E. Leitgeb, ”BER and outage probability of DPSK subcarrier intensity modulated free space optics in fully developed speckle,” *J. Commun.*, vol. 4, no. 8, pp. 546-554, Sep. 2009.

[24] W. O. Popoola, Z. Ghassemlooy, and E. Leitgeb, ”BER performance of DPSK subcarrier modulated free space optics in fully developed speckle,” in *Proc. 2008. CNSDSP*, Graz, pp. 273–277, Jul. 2008.

[25] W. O. Popoola, Z. Ghassemlooy, and E. Leitgeb, ”Free-space optical communication in atmospheric turbulence using DPSK subcarrier modulation,” in *Proc. ISCTA ’07* , 2007.

[26] M. R. Bhatnagar, ”Differential decoding of SIM DPSK over FSO MIMO links,” *IEEE Commun. Lett.*, vol. 17, no. 1, pp. 79–82, Jan. 2013.

[27] Z. Wang, W. D. Zhong, S. Fu and C. Lin, ”Performance comparison of different modulation formats over free-space optical (FSO) turbulence links with space diversity reception technique,” *IEEE Photon. J.*, vol. 1, no. 6, pp. 277–285, Dec. 2009.

[28] X. Song, F. Yang, J. Cheng, N. Al-Dhahir, and Z. Xu, ”Subcarrier phase-shift keying systems with phase errors in lognormal turbulence channels,” *J. Lightw. Technol.*, vol. 33, no. 9, pp. 1896–1904, May 2015.

[29] M. Niu, J. Cheng, and J. F. Holzman, ”Error rate analysis of M-ary coherent free-space optical communication systems with K-distributed turbulence,” *IEEE Trans. Commun.*, vol. 59, no. 3, pp. 664–668, Mar. 2011.

[30] E. Rubiola, *Phase noise and frequency stability on oscillators*. Cambridge University Press, 2008.

[31] I. M. Kostic, *Radio-technique devices and architectures Problems, Solutions and Comments*. Academic Mind, Belgrade, 2013. (in Serbian)

[32] I. Kostic, ”Average SEP for M-ary CPSK with noisy phase reference in Nakagami fading and Gaussian noise,” *Eur. Trans. Telecommun.*, vol. 18, no. 2, pp. 109–113, Mar. 2007.

[33] C. H. Tan and T. T. Tjhung, ”On Fourier Series Expansion of the Phase Density Function,” *IEEE Trans. Commun.*, vol. COM-31, pp. 736-738, May 1983.

[34] I. Kostic, ”Composite phase PDF in gamma shadowed Nakagami fading channel,” *Wireless Pers. Commun.*, vol. 41, no. 4, pp. 465–469, Jun. 2007.

[35] J. W. Matthews, ”On the Fourier coefficients for the phase-shift keyed phase density function,” *IEEE Trans. Inform. Theory*, vol. 21 337–338, May 1975.

[36] G. Lukatela and I. Kostic, ”Analysis of a multilink system in the presence of noise, cochannel interference and some hardware imperfections,” *IEE Proc-F*, vol. 132, no. 6, pp. 511–516, Oct. 1985.

[37] W. C. Lindsey and M. K. Simon, *Telecommunication systems engineering*. Prentice-Hall, 1973.

[38] A. J. Viterbi, *Principles of Coherent Communication*. McGraw-Hill: New York, 1966.

[39] M. K. Simon and M.−S. Alouni, *Digital Communication over Fading Channels*. 2nd ed., New York: John Wiley & Sons Inc., 2004.

[40] J. G. Proakis, *Digital Communications*. 4th ed., New York: McGraw-Hill, Inc., 2001.

[41] L. C. Andrews and R. N. Philips, *Laser Beam Propagation Through Random Media*, 2nd ed., Bellingham, WA, USA: SPIE, 2005.

[42] A. A. Farid and S. Hranilovic, ”Outage capacity optimization for free space optical links with pointing errors,” *J. Lightw. Technol.*, vol. 25, no. 7, pp. 1702–1710, Jul. 2007.

[43] H. G. Sandalidis, ”Optimization models for misalignment fading mitigation in optical wireless links,” *IEEE Commun. Lett.*, vol. 12, no. 5, pp. 395–397, May 2008.

[44] A. A. Farid and S. Hranilovic, ”Outage capacity for MISO intensity-modulated free-space optical links with misalignment,” *IEEE/OSA J. Opt. Commun. Netw.*, vol. 3, no. 10, pp. 780–789, Oct. 2011.

[45] S. Arnon, ”Effects of atmospheric turbulence and building sway on optical wireless-communication systems,” *Opt. Lett.*, vol. 28, no. 2, pp. 129–131, Jan. 2003.

[46] G. Proakis, M. Salehi, and G. Bauch, *Contemporary communication systems using MATLAB®*. 3rd ed., Cengage learning, USA, 2013.

[47] I. S. Gradshteyn and I. M. Ryzhik, *Table of Integrals, Series, and Products*. 6th ed., New York, USA: Academic, 2000.

[48] M. Abramowitz and I. A. Stegun, *Handbook of Mathematical Functions with Formulas, Graphs and Mathematical Tables*. National Bureau of Standards Applied Mathematics Series, Vol. 55, US Government Printing Office, Washington, DC, 1964.

[49] The Wolfarm Functions Site, 2008. [Online] Available: http:/functions.wolfarm.com.

[50] V. Prabhu, ”Error-rate considerations for digital phase-modulation systems,” *IEEE Trans. Commun. Technol.*, vol. 17, no. 1, pp. 33–42, Feb. 1969.

[51] I. Kostic, ”Error rates of DCPSK signlas in hard-limited multilink systems with cochannel interference and noise,” *IEEE Trans. Commun.*, vol. 30, no. 1, pp. 222–230, Jan. 1982.

[52] M. C. Jeruchim, P. Balaban, and K. S. Shanmugan, *Simulation of communication systems*. 2nd ed., New York, USA: Kluwer Academic/Plenum Publishers, 2000.

[53] I. Nåsell, “Inequalities for modified Bessel functions,” Mathematics of Computation, vol. 28, no. 125, pp. 253–256, January 1974.

[54] F. W. J. Olver, D. W. Lozier, R. F. Boisvert, and Ch. W. Clark, *NIST Handbook of Mathematical Functions.* Cambridge University Press, New York, 2010.

[55] I. S. Sokolnikoff and R. M. Redheffer, *Mathematics of Physics and Modern Engineering.* McGraw-Hill Book Company, Inc., New York, 1958.

[56] G. Dahlquist and Å. Björck, *Numerical Methods in Scientific Computing.* Vol. I, SIAM, Philadelphia, 2008.

This article has been accepted for publication in a future issue of this journal, but has not been fully edited. Content may change prior to final publication. Citation information: DOI 10.1109/TWC.2017.2711004, IEEE Transactions on Wireless Communications

Milica I. Petkovic was born in Knjazevac, Serbia, in 1986. She received her M.Sc. and Ph.D. degrees in electrical engineering from the Faculty of Electronic Engineering, University of Nis, Serbia, in 2010, and 2016, respectively. Currently, she is a Research Assistant at the Department of Telecommunications, Faculty of Electronic Engineering, University of Nis, Serbia.

Her research interests include communication theory, wireless and optical communication systems, application of different modulation techniques and modeling of fading channels. Her Ph.D degree is in the field of free-space optical systems. She has published several papers on the above subjects.

Goran T. Djordjevic was born in Nis, Serbia. He received his Dipl.Ing., M.S., and Ph.D. degrees in electrical engineering from the Faculty of Electronic Engineering, University of Nis, Serbia, in 1996, 1999 and 2005, respectively. He is a Professor at the Department of Telecommunications, Faculty of Electronic Engineering, University of Nis, Serbia. He teaches courses of Communication Theory, Modeling and Simulation of Communication Systems, Information Theory and Satellite Communications.

His area of interest is communication theory and applications in satellite, wireless and optical communication systems. His current research interests include application of different modulation formats and error control codes in free space optical systems, modeling and simulation of fading channels, as well as synchronization problems. He has published more than 40 high-ranked journal and 150 conference papers. He is an author of two books (in Serbian) in the field of communication theory.

George K. Karagiannidis was born in Pithagorion, Samos Island, Greece. He received the University Diploma (5 years) and PhD degree, both in electrical and computer engineering from the University of Patras, in 1987 and 1999, respectively. From 2000 to 2004, he was a Senior Researcher at the Institute for Space Applications and Remote Sensing, National Observatory of Athens, Greece. In June 2004, he joined the faculty of Aristotle University of Thessaloniki, Greece where he is currently Professor in the Electrical & Computer Engineering Dept. and Director of Digital Telecommunications Systems and Networks Laboratory. He is also Honorary Professor at South West Jiaotong University, Chengdu, China.

His research interests are in the broad area of Digital Communications Systems and Signal processing, with emphasis on Wireless Communications, Optical Wireless Communications, Wireless Power Transfer and Applications, Molecular and Nanoscale Communications, Stochastic Processes in Biology and Wireless Security.

He is the author or co-author of more than 400 technical papers published in scientific journals and presented at international conferences. He is also author of the Greek edition of a book on "Telecommunications Systems" and co-author of the book "Advanced Optical Wireless Communications Systems", Cambridge Publications, 2012.

Dr. Karagiannidis has been involved as General Chair, Technical Program Chair and member of Technical Program Committees in several IEEE and non-IEEE conferences. In the past, he was Editor in IEEE Transactions on Communications, Senior Editor of IEEE Communications Letters, Editor of the EURASIP Journal of Wireless Communications & Networks and several times Guest Editor in IEEE Selected Areas in Communications. From 2012 to 2015 he was the Editor-in Chief of IEEE Communications Letters.

Dr. Karagiannidis is IEEE Fellow and one of the highly-cited authors across all areas of Electrical Engineering, recognized as 2015 and 2016 Thomson Reuters highly-cited researcher.

Gradimir V. Milovanovic is a Professor of Numerical Analysis and Approximation Theory and Full Member of the Serbian Academy of Sciences and Arts. He studied at University of Nis, obtaining a B.Sc. (1971) in electrical engineering and computer sciences and an M.Sc. (1974) and a Ph.D. (1976) in mathematics.

He was with the Faculty of Electronic Engineering and the Department of Mathematics at the same place as, promoted to professor (1986) and acting as Dean of the Faculty of Electronic Engineering (2002-2004) and Rector of the University of Nis (200406), as well as Dean of the Faculty of Computer Sciences at the Megatrend University, Belgrade (2008-2011), until he joined the Mathematical Institute of the Serbian Academy of Sciences and Arts in Belgrade (2011). He was President of the National Council for Scientific and Technological Development of the Republic of Serbia (2006-2010).

His research interests are in applied and computational mathematics, with emphasis on theory of orthogonality and interpolation and quadrature processes, as well as applications in communication theory (Home page: http://www.mi.sanu.ac.rs/ gvm/). He is currently serving as an Editor-in-Chief and an Associate Editor for several journals (*Journal of Inequalities and Applications*, Springer; *Optimization Letters*, Springer; *Applied Mathematics and Computation*, Elsevier; *Publications de l'Institut Mathmatique*, Mathematical Institute, Belgrade, etc.). He is a co-author of the monographs "*Topis in Polynomials: Extremal Problems, Inequalities, Zeros*" (World Scientific, 1994) and "*Interpolation Processes - Basic Theory and Applications*" (Springer, 2008).